

## Framework coordination of single-ion Cu<sup>2+</sup> sites in hydrated <sup>17</sup>O-ZSM-5 zeolite

Arianna Actis<sup>1</sup>, Enrico Salvadori<sup>1,\*</sup>, Mario Chiesa<sup>1\*</sup>

<sup>1</sup>Department of Chemistry and NIS Centre, University of Torino, Via Giuria 7, 10125 Torino (Italy)

\*Corresponding authors: [enrico.salvadori@unito.it](mailto:enrico.salvadori@unito.it), [mario.chiesa@unito.it](mailto:mario.chiesa@unito.it)

### Supporting Information

#### Table of contents

X-band CW-EPR spectroscopy: additional data .....	S2
ENDOR spectroscopy: additional information .....	S4
<sup>17</sup> O HYSCORE spectra: <sup>17</sup> O and <sup>27</sup> Al hyperfine couplings .....	S6
References .....	S7

## X-band CW-EPR spectroscopy: additional data

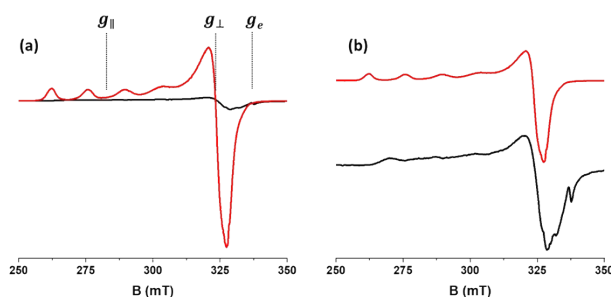


**Fig. S1.** Comparison between the CW EPR spectra of Cu-<sup>17</sup>OZSM-5-H<sub>2</sub><sup>16</sup>O recorded before (black) and after (red) hydration. Panel (a) reports the raw data and shows the well-known signal enhancement brought about by the coordinating water molecules. As point of reference, the positions corresponding to  $g_{\parallel}$ ,  $g_{\perp}$  and  $g_e$  (2.0023) are also reported to demonstrate that the SOMO orbital always mostly comprises the  $d_{x^2-y^2}$  Cu atomic orbital ( $g_{\parallel} > g_{\perp} > g_e$  and  $A_{\parallel} > A_{\perp}$ ). Panel (b) shows a comparison between the same spectra normalised. As it can be clearly seen from panel (b) the Cu hyperfine couplings do not vary dramatically upon hydration/dehydration and therefore are not informative about the electronic structure and binding mode.

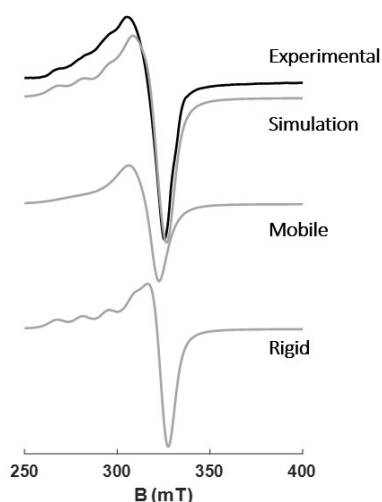


**Fig. S2** Comparison between the experimental X-band CW-EPR spectrum of Cu-<sup>17</sup>OZSM-5-H<sub>2</sub><sup>16</sup>O recorded at 298 K and its best global simulations. Individual components corresponding to the spin-Hamiltonian parameters reported in Table S1 are also reported.

To quantitatively account for the qualitative observations reported in the main text, the spectra were simulated to extract the spin-Hamiltonian parameters considering a single species at 77 K and two distinct species at 298 K, one rigid and one mobile. For the latter a characteristic correlation time of  $2.5 \times 10^{-10}$  s can be estimated (see Supporting Information Figure S2). Spectra simulations reveal that in all cases  $g_{\parallel} > g_{\perp} > g_e$  and  $A_{\parallel} \gg A_{\perp}$  implying a Singly Occupied Molecular Orbital (SOMO) mostly comprised of the  $d_{x^2-y^2}$  Cu<sup>2+</sup> orbital.

	$g_{\parallel}$	$g_{\perp}$	$ A_{\parallel} $	$ A_{\perp} $	Correlation time	Weight
<b>298 K</b>						
Mobile species	$2.40 \pm 0.03$	$2.10 \pm 0.02$	$360 \pm 40$	$80 \pm 20$	$2.5 \times 10^{-10} \pm 0.6 \times 10^{-10}$	60%
Rigid species	$2.345 \pm 0.005$	$2.09 \pm 0.01$	$444 \pm 40$	$20 \pm 5$	/	40%
<b>77K</b>						
Rigid species	$2.386 \pm 0.002$	$2.079 \pm 0.002$	$444 \pm 10$	$20 \pm 5$	/	100%

**Table S1.** Spin Hamiltonian parameters extracted from simulation of hydrated Cu-ZSM5 at room temperature. All hyperfine interactions are given in units of MHz, whereas the correlation time is given in unit of s.

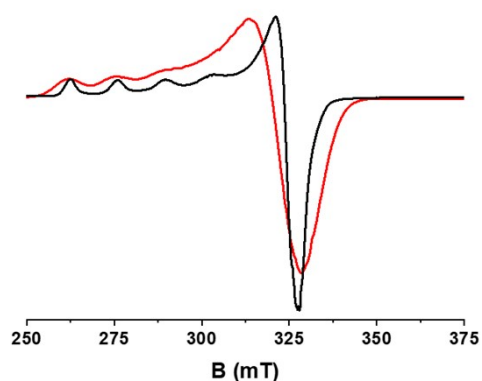


**Fig. S3** Comparison between the experimental X-band CW-EPR spectra of Cu-<sup>17</sup>OZSM-5-H<sub>2</sub><sup>16</sup>O (black) and Cu-<sup>16</sup>OZSM-5-H<sub>2</sub><sup>17</sup>O (red) recorded at 77 K. A considerable line broadening due to the H<sub>2</sub><sup>17</sup>O solvating water is clearly distinguishable.

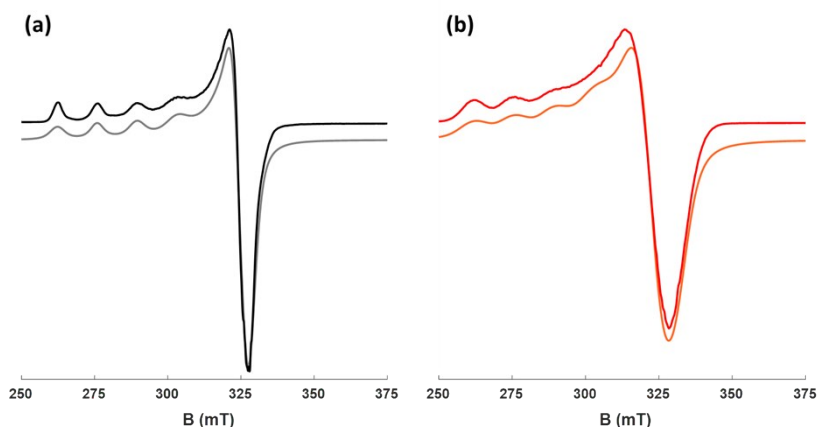


**Fig. S4** Comparison between the experimental X-band CW-EPR spectrum of Cu-<sup>17</sup>OZSM-5-H<sub>2</sub><sup>16</sup>O (a) Cu-<sup>16</sup>OZSM-5-H<sub>2</sub><sup>17</sup>O (b) recorded at 77 K and their simulations grey and orange lines, respectively. The simulation in (a) corresponds to the spin-Hamiltonian parameters reported in Table S1, while the simulation in (b) considers the same spin-Hamiltonian parameters as well as the <sup>17</sup>O hyperfine coupling constants derived from <sup>17</sup>O ENDOR spectroscopy (See Figure 3 and Table 1 main text for reference).

## ENDOR spectroscopy: additional information

<b>Cu-<sup>16</sup>OZSM-5-H<sub>2</sub><sup>17</sup>O</b>				
<b>Magnetic Field (mT)</b>	<b><i>g</i></b>	<b>Larmor frequency <sup>1</sup>H (MHz)</b>	<b>Larmor frequency <sup>17</sup>O (MHz)</b>	<b>Working frequency (GHz)</b>
995.0	2.427	42.36	5.75	33.88012
1005.0	2.403	42.79	5.80	33.88013
1040.0	2.323	44.28	6.01	33.87955
1080.0	2.236	45.98	6.24	33.87993
1120.0	2.156	47.69	6.47	33.87937
1158.5	2.085	49.33	6.69	33.88018

**Table S2.** Summary of experimental and physical parameters useful for the interpretation of the ENDOR spectra reported in Figure 3a (main text) for the sample Cu-<sup>16</sup>OZSM-5-H<sub>2</sub><sup>17</sup>O.

<b>Cu-<sup>17</sup>OZSM-5-H<sub>2</sub><sup>16</sup>O</b>				
<b>Magnetic Field (mT)</b>	<b><i>g</i></b>	<b>Larmor frequency <sup>1</sup>H (MHz)</b>	<b>Larmor frequency <sup>17</sup>O (MHz)</b>	<b>Working frequency (GHz)</b>
1006	2.402	42.83	5.80	33.82446
1020	2.369	43.43	5.89	33.82420
1040	2.323	44.28	6.01	33.82466
1060	2.278	45.13	6.12	33.82403
1080	2.236	45.98	6.24	33.82500
1115	2.167	47.47	6.44	33.81810
1140	2.120	48.54	6.58	33.81826
1160	2.083	49.39	6.70	33.80652

**Table S3.** Summary of experimental and physical parameters useful for the interpretation of the ENDOR spectra reported in Figure 3b (main text) for the sample Cu-<sup>17</sup>OZSM-5-H<sub>2</sub><sup>16</sup>O.

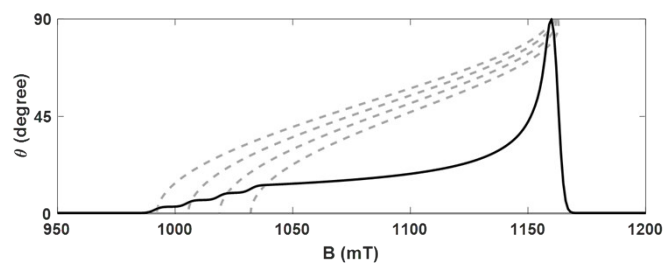


**Fig. S5.** Angular roadmap for a  $\text{Cu}^{2+}$  ion. The Q-band EPR spectrum (black continuous line) represents the powder average over all possible orientations and has been simulated with the spin-Hamiltonian parameters reported in Table S1 for the spectrum recorded at 77 K ( $g_{\parallel} = 2.386$ ,  $g_{\perp} = 2.079$ ,  $|A_{\parallel}| = 444$  MHz,  $|A_{\perp}| = 20$  MHz). The linewidth was set smaller than the experimental to enhance the Cu hyperfine features along  $g_{\parallel}$ . The dashed lines (grey) represent the position of the resonance frequencies for each Cu hyperfine transition as a function of the angle,  $\vartheta$ , between the applied magnetic field,  $B_0$ , and the  $\mathbf{g}$  tensor: for  $\vartheta = 0^\circ$ ,  $g_{\parallel} // B_0$ , whereas for  $\vartheta = 90^\circ$ ,  $g_{\perp} // B_0$ .

## $^{17}\text{O}$ HSCORE spectra: $^{17}\text{O}$ and $^{27}\text{Al}$ hyperfine couplings

**$^{17}\text{O}$  HSCORE.** Previous reports on  $\text{H}_2^{17}\text{O}$  axially coordinate to  $\text{Cu}^{2+}$  ions either in inorganic salts<sup>1</sup> or biological samples<sup>2,3</sup> reported an  $a_{\text{iso}}$  of  $\approx 1\text{MHz}$  and a maximum coupling of  $\approx 3\text{MHz}$ . The most complete dataset obtained for  $\text{Cu}^{2+}$  doped zinc sulfate hexahydrate reports  $a_{\text{iso}} = -1.15\text{MHz}$  and  $A = [1.28, 1.38, -2.66]\text{MHz}^1$ , where the lower hyperfine value for the axial position, as compared to the equatorial position, is due to the larger distance from the nucleus and the unfavorable overlap with the predominant  $d_{x^2-y^2}$  SOMO orbital.  $^{17}\text{O}$  HSCORE on  $\text{Cu-}^{16}\text{OZSM-5-H}_2^{17}\text{O}$  yielded a maximum coupling of  $\approx 1.5\text{MHz}$ , significantly lower than the expected value, suggesting either a square pyramidal coordination (where the bond length of fifth, apical ligand is longer than usual) or square planar geometry.

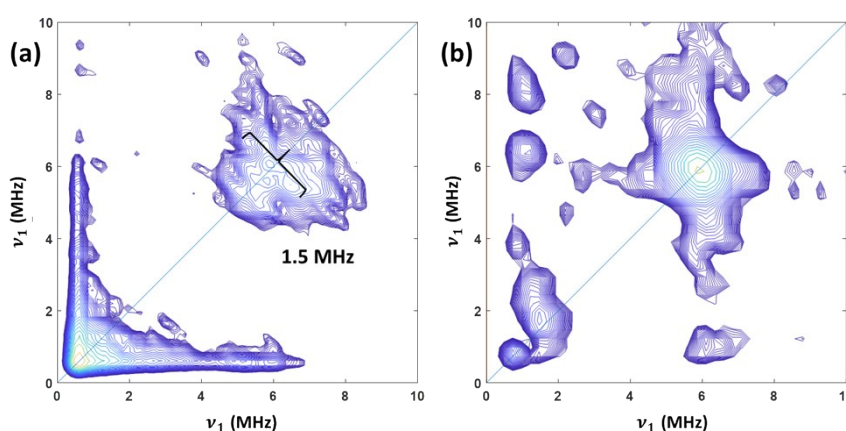


**Fig. S6** Comparison between the experimental Q-band  $^{17}\text{O}$  HSCORE spectra obtained for (a)  $\text{Cu-}^{16}\text{OZSM-5-H}_2^{17}\text{O}$  at 1035.1 mT (b)  $\text{Cu-}^{17}\text{OZSM-5-H}_2^{16}\text{O}$  at 1019.8 mT. Estimates of the relevant  $^{17}\text{O}$  hyperfine couplings are indicated in (a), whereas no appreciable  $^{17}\text{O}$  hyperfine coupling could be measured in (b). HSCORE spectra recorded at 10 K and with a  $\tau$  value of 166 ns (a) and 132 ns (b).

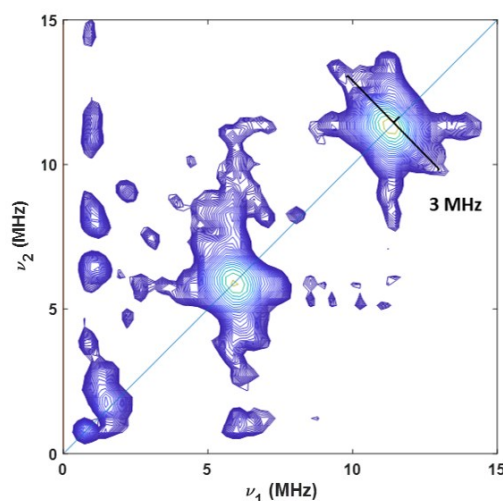


**Fig. S7** Extended Q-band HSCORE spectrum for  $\text{Cu-}^{17}\text{OZSM-5-H}_2^{16}\text{O}$  recorded at 1019.8 mT and  $\tau = 132\text{ns}$ . A  $^{27}\text{Al}$  coupling of  $\approx 3\text{MHz}$  can be estimated, in line with previously reported values for other  $\text{Cu}^{2+}$  loaded zeolite systems<sup>4,5,6</sup>.

## References

---

1. M. J. Colaneri, J. Vitali, Probing Axial Water Bound to Copper in Tutton Salt Using Single Crystal  $^{17}\text{O}$ -ESEEM Spectroscopy, *J. Phys. Chem. A*, 2018, **122** (30), 6214–6224
2. M. O. Ross, F. MacMillan, J. Wang, A. Nisthal, T. J. Lawton, B. D. Olafson, S. L. Mayo, A. C. Rosenzweig, B. M. Hoffman, Particulate methane monooxygenase contains only mononuclear copper centers, *Science*, 2019, **364**, 566–570
3. D. Kim, N. H. Kim, S. H. Kim, 34 GHz Pulsed ENDOR Characterization of the Copper Coordination of an Amyloid  $\beta$  Peptide Relevant to Alzheimer's Disease, *Angew. Chem. Int. Ed.*, 2013, **52**, 1139–1142
4. D. Goldfarb, L. Kevan,  $^{27}\text{Al}$  fourier-transform electron-spin-echo modulation of  $\text{Cu}^{2+}$ -doped zeolites A and X, *J. Mag. Res.*, 1989, **82** (2), 270-289
5. D. Goldfarb, K. Zukerman, Characterization of  $\text{Cu}^{2+}$  sites in zeolites NaX and KX by  $^{27}\text{Al}$  electron spin echo envelope modulation, *Chem. Phys. Lett.*, 1990, **171** (3), 167-174
6. P. J. Carl, D. E. W. Vaughan, D. Goldfarb, Interactions of  $\text{Cu}(\text{II})$  Ions with Framework Al in High Si:Al Zeolite Y as Determined from X- and W-Band Pulsed EPR/ENDOR Spectroscopies, *J. Phys. Chem. B*, 2002, **106** (21), 5428–5437